research articles Journal of proteome research

Diversity of cAMP-Dependent Protein Kinase Isoforms and Their Anchoring Proteins in Mouse Ventricular Tissue

Arjen Scholten,[†] Toon A. B. van Veen,[‡] Marc A. Vos,[‡] and Albert J. R. Heck*[,†]

Department of Biomolecular Mass Spectrometry, Bijvoet Center for Biomolecular Research and Utrecht Institute for Pharmaceutical Sciences, Utrecht University, Sorbonnelaan 16, 3584 CA Utrecht, the Netherlands, and Department of Medical Physiology, University Medical Center Utrecht, A. Numan Building, 4th floor, Yalelaan 50, 3584 CM Utrecht, The Netherlands

Received November 15, 2006

Using a chemical proteomics approach, we efficiently enriched for the generally low abundant cAMP signaling proteins, and their interactors, directly from mouse ventricular tissue. The presence of undesired contaminating (noncyclic) nucleotide-binding proteins was diminished using a tailored sequential elution protocol. Through further optimization of this affinity purification and elution protocol, we were able to detect all known protein kinase A regulatory isoforms (PKA-R). Furthermore, 11 different A-kinase anchoring proteins (AKAPs) were detected. A proposed fusion protein of paralemmin 2 and AKAP2 could be decisively established as a novel AKAP at the protein level in ventricular tissue. When comparing this dataset of cAMP-affinity purified proteins with earlier data obtained with immobilized cGMP from rat ventricular tissue, we observe a large overlap in the retained proteins but also some clear differences. Furthermore, implementation of an in-depth analysis of *in vivo* phosphorylation sites on PKA-R revealed the presence of several differentially phosphorylated PKA-R isoforms. This illustrates yet another layer of functional regulation in cyclic nucleotide signaling. In general, our improved chemical proteomics screen offers a broad, but detailed, view on nature's complex diversity in cyclic nucleotide signaling mechanisms. Possibly different AKAP-isoforms may direct differentially phosphorylated PKA-R isoforms to different cellular compartments, providing a multifaceted platform for just this kinase.

Keywords: PALM2-AKAP2 • cAMP • PKA • chemical proteomics • ventricular tissue • phosphorylation

Introduction

The cyclic nucleotide cAMP (adenosine-3′,5′-cyclic monophosphate) plays a pivotal role in the regulation of many functions in a multitude of cell types. This regulation is primarily achieved by activating the cAMP-regulated protein kinase (PKA). Cellular levels of cAMP increase following extracellular stimulation of different G-protein coupled receptors (GPCRs). Upon stimulation, the inactive heterotetrameric PKA (R_2C_2) dissociates into a dimer of two cAMP-bound regulatory domains (PKA-R or R_2) and two separate catalytic subunits (PKA-C or 2C). When intracellular cAMP levels drop, cAMP dissociates from PKA-R. This enables it to bind PKA-C again, thereby inactivating kinase activity.[1] PKA is involved in many signaling pathways, often taking place within different compartments of one cell. Therefore, strong spatial regulation of PKA is essential. This is achieved by binding of PKA to a distinct group of proteins called A-kinase anchoring proteins, or AKAPs.[2] The highly diverse members of the AKAP protein family localize to various compartments of the cell and form the basis of PKA's spatial regulation.

Here we study specifically PKA-R and its interacting partners in heart ventricular tissue of the mouse. Within the cardiovascular system, the cAMP-pathway is important in the sympathetic regulation through β-adrenergic stimuli. PKA is known to phosphorylate, among others, Troponin I,[3,4] L-type Ca^{2+} channels (also called dihydropyridine receptor (DHPR)),[5] and the ryanodine receptor (RyR).[6] As in other tissues, the activity of PKA within the cardiovascular system requires the involvement of AKAPs. For instance, for cardiac contractility, PKA-AKAP complex formation is crucial.[7] AKAPs whose function is more or less well defined in the cardiovascular system are AKAP9 (Yotiao),[8] AKAP7α (AKAP15/18),[9,10] and AKAP6 (mAKAP).[11] These three AKAPs each have a strong influence on intracellular cation concentrations, regulated through ion channels. AKAP7α and AKAP6 influence intracellular Ca^{2+} concentration,[9−11] whereas Yotiao was found to target PKA RII and the phosphatase PP1 to the KCNQ1 channel to regulate intracellular potassium ion levels.[8] Eleven other AKAPs have been reported to be present in heart tissue or cardiomyocytes.[12]

A related second messenger in the cardiovascular system is cGMP (guanosine-3′,5′-cyclic monophosphate). cGMP stimu-

* To whom correspondence should be addressed. Albert J. R. Heck, Utrecht University, Sorbonnelaan 16, 3584 CA, Utrecht, The Netherlands; Tel, +31 (0)30 253 6797; Fax, +31 (0)30 251 8219; E-mail, a.j.r.heck@uu.nl.
† Utrecht University.
‡ University Medical Center Utrecht.

10.1021/pr060601a CCC: $37.00

Published on Web 04/14/2007

lates the cGMP-dependent protein kinase (PKG), which is the closest related kinase to PKA. Although PKG is primarily activated by cGMP, it also binds to cAMP.[13,14] It has been suggested that cGMP and cAMP can activate each others' kinases.[15] This direct link between PKA and PKG hampers, to some degree, the study of these proteins individually, as dissecting the individual pathways of PKA and PKG requires specific inhibitors.[16]

Compared to the major house-keeping proteins, PKA and its AKAPs are not highly abundant in heart tissue, and therefore they are often not, or only marginally, detected in global proteomic surveys. This is primarily due to the limited dynamic range in analyzing simultaneously high and low abundant proteins by mass spectrometry-based proteomic screens. This may be regarded as one of the major current bottle-necks of the technique. To overcome these limitations, subproteomic approaches can be used, selectively isolating for instance cellular organelles or proteins of particular subclasses.

Here we further exploit such a chemical proteomics[17−19] approach using immobilized cAMP to enrich, isolate, and detect PKA and its low abundant interaction partners, like AKAPs, directly from a crude lysate of mouse ventricular tissue. A tailored sequential elution protocol, based on previous experience, enabled us to separate to a large degree the pathways involving cGMP and cAMP. At the same time, the binding of less specific, albeit more abundant, proteins, such as general noncyclic nucleotide binding proteins, could be diminished. A very specific enrichment of PKA-R and several interacting AKAPs directly from the mouse ventricular tissue sample was achieved. The proteins in the highly enriched fraction were separated, identified, and analyzed in detail using 1D gel separation followed by nanoflow LC−LTQ−FTICR mass spectrometry. We were able to obtain good sequence coverage of several cAMP-signaling proteins among which were all known PKA regulatory subunit isoforms. On these we additionally detected distinguishable phosphorylation patterns. Furthermore, we detected 11 different AKAPs. When we compare earlier data from rat ventricular tissue[20] with this dataset, clear overlaps and differences are observed. Interestingly, the repertoire of AKAPs was found to be further diversified by the presence of multiple splice variants, including a novel fusion protein. Our data provide a broad view on the elegant multifaceted aspects of cAMP/PKA signaling. This encompasses a variety of differentially phosphorylated isoforms of PKA-R, several AKAPs, and their specific isoforms. The different isoforms may lead to different functional interactions and different cellular locations.

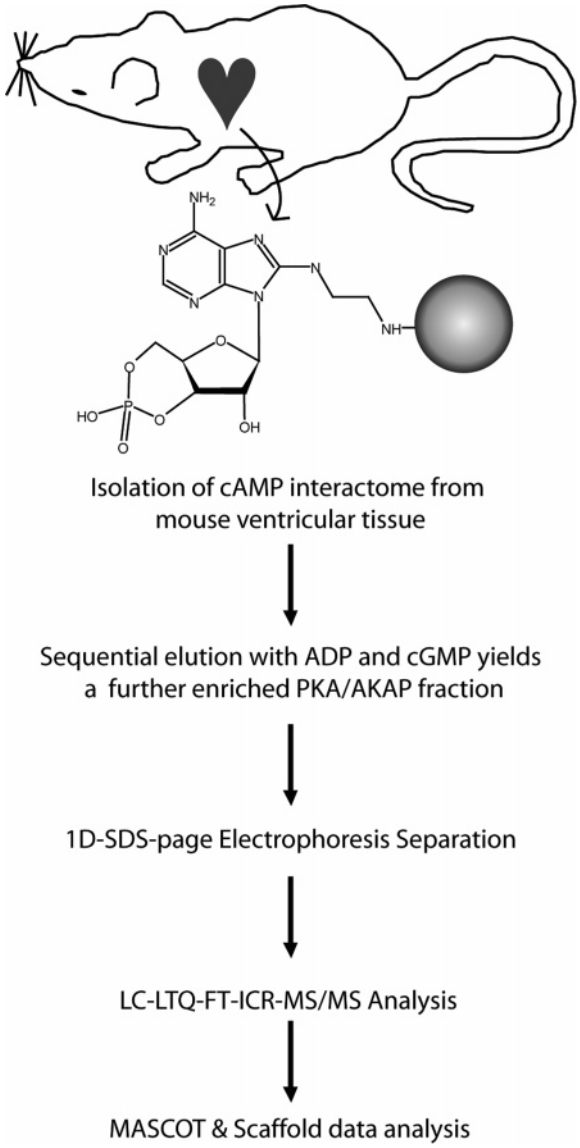

Figure 1. Outline of the experimental protocol. Excorporated mouse ventricular tissue was solubilized and treated with 8AEA-cAMP agarose beads. After washing, the cAMP-interactome that was present on the beads was further enriched by sequential elution with ADP and cGMP to yield a concentrated final fraction of PKA and several different AKAPs. The three protein fractions were separated by SDS-PAGE gel electrophoresis and subsequently identification of proteins present in each fraction was attained by LC−LTQ−FTICR−MS/MS and MASCOT and Scaffold searches.

Materials and Methods

Materials. All chemicals were purchased from commercial sources and were of analysis grade. Agarose affinity beads: 8-(2-aminoethyl)aminoadenosine-3′,5′-cyclic monophosphate (8AEA-cAMP, see also Figure 1) were provided by Biolog. Protease inhibitor cocktail (Complete Mini) and trypsin (sequencing grade) were obtained from Roche. HPLC-S gradient grade acetonitrile (AcN) was purchased from Biosolve and high purity water (MQ) obtained from a Milli-Q system (Millipore) was used in all experiments.

Sample Preparation. Hearts from adult FVB/N mice (4−6 months old) were excorporated, frozen in liquid nitrogen, and stored at −80 °C until use. For protein isolation, the ventricular tissue of two mice was combined, cooled with liquid nitrogen, and pulverized in a custom-made mortar which was also precooled with liquid nitrogen. The powdered tissue was than transferred to 1 mL of ice-cold PBS−TS (50 mM KPO_4, 150 mM NaCl, 0.1% Tween 20, 300 mM sucrose) and left at RT for 5 min. Subsequently, samples were stored on ice for another 10 min and centrifuged at 20 000 g in a table top Eppendorf centrifuge (Eppendorf) at 4 °C. The obtained soluble fraction (20 mg of total protein) was carefully collected and diluted to a protein concentration of 3 mg mL^{-1} in lysis buffer before addition of 50 μL (dry volume) of 8-AEA-cAMP affinity beads (cAMP-density of 6 μmol mL^{-1}). The lysate-beads suspension was left at 4 °C under agitation for 2 h. The beads were washed 6 times in cold PBS−TS with a total beads-to-washing volume ratio of 4×10^7. The beads were subsequently subjected to 50 μL of 10 mM ADP (3×), 500 μL of PBS−TS, 50 μL of 5 mM cGMP

(3×), and again 500 μL of PBS−TS before addition of gel loading buffer and heating at 95 °C for 5 min. The three ADP and cGMP fractions were combined and concentrated to a volume of ∼15 μL using Ultrafree-0.5 centrifugal filter units (5 kDa molecular weight cutoff) (Millipore, Bedford MA) before addition of gel loading buffer and heating at 95 °C for 5 min. Protein fractions were separated by 12% acrylamide SDS page electrophoresis and visualized by colloidal Coomassie staining.

Protein Identification. Each of the 1D gel lanes was cut into 19 pieces. Gel pieces were subsequently washed with MQ and AcN. Proteins were in-gel digested using a protocol adapted from Wilm et al.[21] Briefly, gel pieces were reduced in 1,4-dithiothreitol (6.5 mM) and alkylated with iodoacetamide reagent (54 mM). After thorough washing, pieces were rehydrated in trypsin solution (10 ng/μL) on ice. After addition of 30 μL Na_2CO_3 (50 mM, pH 8.5), samples were digested overnight at 37 °C. Supernatant of the digest was collected. The gel pieces were washed for 30 min in 5% formic acid at RT, after which the supernatant of this washing step was combined with the earlier fraction and stored at −30 °C until analysis.

For analysis, digested samples (20 μL) were thawed and injected onto an Agilent 1100 HPLC system (Agilent Technologies) reconfigured into a nanoscale liquid chromatography system.[22,23] This LC-system was coupled to a 7-Tesla Finnigan LTQ−FTICR mass spectrometer (Thermo Electron) equipped with a nanoflow electrospray ion source. Briefly, the mass spectrometer was operated in the data-dependent mode to automatically switch between MS and MS/MS acquisition. Survey full scan MS spectra (from m/z 300−1500) were acquired in the FTICR with resolution $R = 25\,000$ at m/z 400 (after accumulation to a target value of 5×10^6 in the linear ion trap). The three most intense ions were sequentially isolated for accurate mass measurements by a FTICR "SIM scan" over a 15 Da mass range, $R = 50\,000$ and target accumulation value of 8×10^4. These ions were fragmented in the linear ion trap using collisionally induced dissociation at a target value of 1×10^4.

Semiquantitative Data Analysis. The mass spectrometric data was analyzed using MASCOT (www.matrixscience.com) and Scaffold (www.proteomesoftware.com). The IPI-mouse database, version 3.11, was searched with 10 ppm accuracy on the precursor mass and 0.9 Da on the tandem MS data. Variable modifications included were methionine oxidation and serine/threonine phosphorylation. Final results were obtained by setting a 95% confidence level on the peptide and protein identification in Scaffold. Only proteins with a minimum of three unique peptides were considered. Scaffold was used to eliminate redundancy and to assign individual proteins to the particular gel piece in which most unique peptides were found. Proteins were classified according to their nucleotide binding properties using the online Swiss-Prot protein database (www.expasy.org) or by additional literature searches.

To semiquantitate the abundance of proteins in each of the eluted fractions, we developed a protocol using the number of peptide queries as an estimate for protein abundance. As evidently large proteins may give rise to more peptides than small proteins, we introduced a molecular weight related correction. Similar semiquantitative approaches based on the amount of (unique) queries have been described.[24,25] We use a semiquantitative abundance factor, F_{abb},[20] by taking for each individual protein the ratio between the molecular weight and the amount of peptide queries (MW/queries). The lower F_{abb}, the more abundant the protein is. Comparison of these F_{abb} factors for proteins in different eluted fractions indicated the relative abundance of each protein in these fractions.

Analysis of Protein Phosphorylation. For the analysis of phosphopeptides, we implemented serine and threonine phosphorylation as variables in MASCOT. All peptides identified by their MS/MS-spectra as originating from phosphopeptides were manually inspected and compared to their nonphosphorylated counterparts (if present). To estimate the stoichiometry of phosphorylation at specific sites, single ion chromatograms (SICs) were created of all peptides for the phosphorylated form, as well as the nonphosphorylated form. This was done for all observed charge states and with a mass window of 0.02 Da around the observed mass. The SIC-quantitation depends heavily on ionization efficiency in the MS-survey scan. These efficiencies are by definition different for each peptide, even for differential post-translationally modified peptides. Therefore, we only semiquantitated the relative phosphorylation stoichiometries by comparing peak intensities.

Results and Discussion

Specific Elution Yields Distinct Protein Fractions. In chemical proteomics, it is of utmost importance that the compound of interest is immobilized to the bead without compromising the binding properties of the compound. For the investigation of cAMP-interacting proteins, there are several choices to link the cAMP molecule to the bead, as described previously in detail.[20,26] In the present experiments, we used 8-AEA-cAMP-Agarose beads (see Figure 1) to enrich for cAMP-binding proteins and their binding partners. As expected, our cAMP-affinity pull-down was contaminated with high abundant, albeit less specific binding proteins. Therefore, a tailored sequential elution protocol was developed to obtain a distinct protein fraction enriched in PKA-R and AKAPs. The protocol consisted of an ADP and a cGMP elution to have the highly enriched PKA-R/AKAP fraction left on the beads. Proteins in all fractions were separated and visualized by 1D gel electrophoresis, as shown in Figure 2. The proteins present in the ADP-fraction and cGMP fraction are depicted in lane 2 and 3 of Figure 2, respectively. Final elution of the PKA-R/AKAP fraction from the beads was achieved by addition of SDS-PAGE loading buffer, lane 4. Lanes 2, 3, and 4 were each cut into 19 equal gel pieces. Following trypsin digestion, proteins were identified using a nanoLC−LTQ−FTICR−MS/MS as described previously.[27] The resulting mass spectra were analyzed using MASCOT and Scaffold software packages.[28,29] Only proteins that were identified with at least 3 unique peptides, with a MASCOT peptide score of 29 ($p < 0.05$) or higher, were considered. Using these stringent criteria, we identified 96 proteins in the ADP fraction, whereas 16 and 62 proteins were detected in the cGMP and final-enriched fraction, respectively (Table 1A−C). By comparing the three gel lanes, we can conclude that the ADP elution efficiently removed less specific noncyclic nucleotide binding proteins, whereas the cGMP elution performed well in separating PKG from PKA-R.

Estimation of Protein Abundance in the Different Fractions. The SDS-PAGE gel in Figure 2 illustrates that the elution protocol provides three distinct protein fractions. Nonetheless, we observed that quite a few proteins were detected in all three fractions (see Table 1 and Supplemental Table 1, Supporting Information). To estimate the relative abundance of these proteins in the different fractions, we first looked at the intensities of the silver-stained bands of specific proteins in the different elutions. The gel intensity was normalized to the

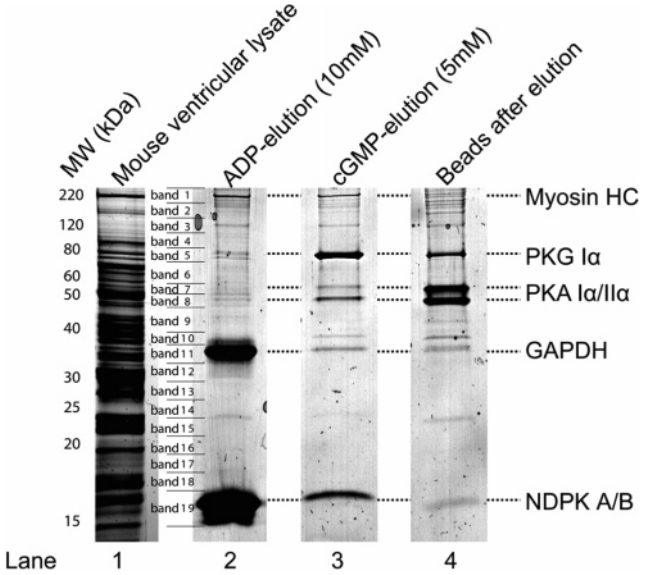

Figure 2. Sequential elution yields distinct protein fractions. SDS-PAGE gel of mouse ventricular tissue (lane 1) treated with 8-AEA-cAMP. Sequential elution with ADP (lane 2) and cGMP (lane 3) yields a final enriched protein fraction highly enriched for PKA and its binding partners (lane 4). The 19 separate gel slices are indicated by Band1-Band19 and are applicable to all three lanes.

most intense band of a particular protein. In Figure 3A, the normalized densitometric detection of protein abundance is given for a few of the high abundant proteins in the pull down. It shows that the majority of captured GAPDH dissociates already during the ADP elution, whereas the majority of PKG can be eluted with cGMP. This gel-staining-based approach is somewhat limited and can only be applied to the most abundant proteins on the gel. Furthermore, proteins that run in the 1D gel at similar apparent molecular weights, including some protein isoforms, cannot easily be treated separately.

To overcome some of these problems, we used Scaffold-based outputs to estimate relative protein abundance and used the amount of mass spectra obtained for a certain protein, now referred to as queries, as an indication of protein abundance.[24,25] Queries of a particular protein in each of the three fractions were normalized to the highest value. The number of queries for each protein in each fraction is listed in Table 1 (and Supplemental Table 1, Supporting Information). The results of this treatment are shown in Figure 3B for over 20 proteins, including several isoforms. For proteins that could be semiquantitated by densitometry, we observe a very good correlation with the MS-based estimation of relative protein abundance (compare 3A and 3B). One clear advantage of the query-based method is the much higher sensitivity of the FTICR−MS compared to the gel staining. Additionally, it allows the individual analysis of proteins that overlap on the 1D gel, including some protein isoforms, like PKA-RIα and PKA-RIβ. By comparing the elution patterns, co-purifying proteins can be evalutated. For instance, the elution pattern of PKG does not match with any of the patterns of the AKAPs, indicating they are not binding partners.

To compare the different proteins in each eluted fraction, we applied the F_{abb} factor, in which the amount of queries for a certain protein is corrected for the molecular weight as described previously.[20,24,25] This gives an estimation of the relative abundance of a protein in this fraction when compared to other proteins in this same fraction.

cAMP-Binding Proteins and AKAPs. The fraction depicted in lane 4 of Figure 2 contained a large variety of cAMP-binding proteins and their secondary binding partners (Table 1C). They were almost found exclusively in this fraction (See Figure 3B and Table 1), which shows that specific elution with ADP and cGMP to remove interfering proteins is not affecting the retention of the targeted proteins on the beads. All proteins dependent on cAMP are highlighted in Table 1C. In the final fraction, all four types of PKA-R, PKA-RIα (B1), RIIα (B2), RIIβ (B6), and RIβ (B43), were identified (Table 1C), all with ample unique peptides and high sequence coverage. The α-isoforms are reported to be more abundant than the β-isoforms in mammalian heart, which is in line with our observations (Table 1C).[30] We do not detect the catalytic domains of PKA, which is as expected as they dissociate from the regulatory domains, upon cAMP binding, or in our case, when PKA-R binds to the beads.

Next to the four PKA-R isoforms we detected several AKAPs, many of them in a variety of isoforms. These AKAPs are discussed below.

Splice Isoform Diversity and Fusion Proteins of AKAP 2. AKAP2 has been reported to be an actin cytoskeletal binding AKAP, with a very specific tissue distribution in the particulate fractions of mouse lung, thymus, cerebellum, and kidney.[31] Interestingly, Dong et al. did not find AKAP2 in the particulate fraction of mouse heart by Western blotting.[31] In contrast, we detected AKAP2 as a high abundant protein in the PKA-R-enriched fraction (B13). For AKAP2, 6 mRNA-splice variants have previously been reported (KL1A, 1B, 2A, 2B, 3A, and 3B). The A-isoforms have an N-terminal extension of 124 amino acids. Types 1, 2, and 3 are distinguished by the length, and specific sequence, of their C-termini, as depicted schematically in Figure 4.

In our quest to identify which AKAP2 isoforms we enriched for, we noted that 33 unique peptides were matched to an 1137 amino acid (AA) entry in the IPI-mouse database that was mysteriously called *Protein* (IPI00649060). Initial BLAST analysis revealed that part of *Protein*'s sequence (AA 245−1119) was nearly identical to the one of AKAP2-KL1A (O54931 (Swiss-Prot)). Sequence alignment showed that *Protein* had an additional 244 N-terminal amino acids and a different sequence at the very C-terminus (AA 1119−1129), as depicted in Figure 4. Detailed comparison of the sequences of *Protein* and the six earlier established AKAP2-isoform entries in the Swiss-Prot database revealed that the sequence differed at three different amino acids (Ser364, Lys508, Pro775), see Supplemental Figure 1 (Supporting Information). Twenty peptides assigned to *Protein* originated from the part of the sequence that is conserved in all six isoforms of AKAP2 (AA 369−1033, Figure 4).[31] We observed one peptide (AA 493−508, see Supplemental Figure 1, Supporting Information) that contained a lysine at position 508 and not an arginine, as predicted in the Swiss-Prot database (see Supplemental Figure 1, Supporting Information). The 20 peptides, including 493−508, were also matched to two other entries in the IPI-mouse database: IPI00336504 (*AKAP2 Isoform 2*) and IPI00648062 (*MKIAA0920,* BLAST analysis[32] showed this to be 100% identical to IPI00336504), indicating a discrepancy between the AKAP2 sequences in the IPI database and the Swiss-Prot database (data not shown). This discrepancy was also observed for Ser364 and Pro775, which were Ile and Thr in the Swiss-Prot database respectively. At the C-terminus, we observed another peptide (AA 1117−1123) that was matched to *Protein*, IPI00336504, and IPI00648062,

Table 1. Identified Proteins of the 8-AEA-cAMP-Interactome[a]

TABLE 1A Top 20 of proteins in ADP-elution

No	Band	Protein name	MW	Binds	Accession IPI mouse	MASCOT Score	Number of Queries	Unique Spectra	F_{abb}
A1	ADP19	Nucleoside diphosphate kinase B (NDPK B)	17466	AMP/ADP/ATP	IPI00127417	1300	185	26	94
A2	ADP19	Nucleoside diphosphate kinase A (NDPK A)	17311	AMP/ADP/ATP	IPI00131459	1185	126	23	137
A3	ADP11	Glyceraldehyde-3-phosphate dehydrogenase (GAPDH)	35661	NAD/NADH	IPI00462301	2065	206	35	173
A4	ADP02	Myosin heavy chain, cardiac muscle alpha isoform (MHC)	223553	AMP/ADP/ATP	IPI00129404	8077	213	124	1050
A5	ADP19	Nucleoside diphosphate kinase 3 (NDPK3)	19081	AMP/ADP/ATP	IPI00125450	547	14	10	1363
A6	ADP18	Myosin regulatory light chain 2, ventricular/cardiac muscle	18734	Myosin	IPI00555015	403	12	8	1561
A7	ADP12	L-lactate dehydrogenase A chain	36350	NAD/NADH	IPI00319994	726	21	13	1731
A8	ADP15	Myosin light polypeptide 3	22273	Myosin	IPI00133392	634	11	10	2025
A9	ADP09	Actin, alpha skeletal/cardiac/smooth muscle	42034	AMP/ADP/ATP	IPI00114593 IPI00117043 IPI00110827 IPI00480406	752	20	16	2102
A10	ADP11	Fructosamine-3-kinase	35015	GAPDH	IPI00111519	448	16	9	2188
A11	ADP06	Heat shock cognate 71 kDa protein	70855	AMP/ADP/ATP	IPI00323357	1309	26	18	2725
A12	ADP06	Trifunctional protein, α-subunit	82627	CoA	IPI00223092	1263	29	21	2849
A13	ADP07	60 kDa heat shock protein	60939	AMP/ADP/ATP	IPI00308885 IPI00461249	885	21	17	2902
A14	ADP09	3-ketoacyl-CoA thiolase, mitochondrial	41840	CoA	IPI00226430 IPI00653158	614	14	10	2989
A15	ADP06	cGMP-dependent protein kinase type Iα (PKG Iα)	76336	cGMP	IPI00458024	844	24	18	3181
A16	ADP06	Stress-70 protein	73511	AMP/ADP/ATP	IPI00133903	1185	23	19	3196
A17	ADP08	ATP synthase α-chain	59736	AMP/ADP/ATP	IPI00652604 IPI00130280	955	18	15	3319
A18	ADP17	Alpha crystallin B-chain	20051	Actin/Cytoskel.	IPI00138274	248	6	5	3342
A19	ADP18	Nucleoside diphosphate kinase 4 (NDPK 4)	20531	AMP/ADP/ATP	IPI00125448 IPI00620572	148	6	4	3422
A20	ADP08	Dihydrolipoyllysine-residue succinyltransferase	48977	CoA	IPI00134809	376	14	7	3498

TABLE 1B Proteins in cGMP-elution (>3 unique peptides)

No	Band	Protein name	MW	Binds	Accession IPI mouse	MASCOT Score	Number of Queries	Unique Spectra	F_{abb}
G1	**cG6**	**cGMP-dependent protein kinase type Iα (PKG Iα)**	**76336**	**cGMP**	**IPI00458024**	**3599**	**256**	**70**	**298**
G2	cG19	Nucleoside diphosphate kinase B (NDPK B)	17466	AMP/ADP/ATP	IPI00127417	712	33	13	529
G3	cG19	Nucleoside diphosphate kinase A (NDPK A)	17190	AMP/ADP/ATP	IPI00131459	588	20	10	860
G4	cG09	cAMP-dependent protein kinase type Iα Regulatory (PKA RIα)	*43158*	cAMP	IPI00119575	1446	33	22	1308
G5	cG08	cAMP-dependent protein kinase type IIα Regulatory (PKA RIIα)	45572	cAMP	IPI00169788	1234	24	17	1899
G6	cG12	Glyceraldehyde-3-phosphate dehydrogenase (GAPDH)	35661	NAD/NADH	IPI00135284 IPI00273646 IPI00458872	706	15	10	2377
G7	cG19	Nucleoside diphosphate kinase 3 (NDPK 3)	19081	AMP/ADP/ATP	IPI00125450	279	7	5	2726
G8	cG15	Myosin light polypeptide 3	22273	Myosin	IPI00133392	373	8	7	2784
G9	cG17	Myosin regulatory light chain 2, ventricular/cardiac, muscle	18734	Myosin	IPI00555015	283	6	6	3122
G10	cG06	Trifunctional protein, α-subunit	82627	CoA	IPI00223092	993	23	17	3592
G11	cG09	Trifunctional enzyme ß-subunit	51370	CoA	IPI00626102 IPI00115607	448	10	9	5137
G12	cG02	Myosin heavy chain, cardiac muscle alpha isoform (MHC)	223553	AMP/ADP/ATP	IPI00129404	2256	39	34	5732
G13	cG06	Heat shock cognate 71 kDa protein	70855	AMP/ADP/ATP	IPI00323357 IPI00480560	470	8	8	8857
G14	cG10	Actin, alpha skeletal/cardiac/smooth muscle	42034	AMP/ADP/ATP	IPI00114593 IPI00117043 IPI00110827 IPI00480406	299	4	4	10509
G15	cG03	AKAP2 (AKAP-KL)	126072	PKA	IPI00649060	427	9	9	14008
G16	**cG04**	**Epac 2 (RapGEF4, MKIAA4040 protein)**	**115597**	**cAMP**	**IPI00323505 IPI00111748 IPI00623205**	**560**	**9**	**9**	**12844**

TABLE 1C Proteins remaining on beads (>3 unique peptides)

No	Band	Protein name	MW	Binds	Accession IPI mouse	MASCOT Score	Number of Queries	Unique Spectra	F_{abb}
B1	Bead08	**cAMP-dependent protein kinase type Iα Regulatory**	*43158*	cAMP	IPI00119575	1950	167	35	258
B2	Bead07	**cAMP-dependent protein kinase type IIα Regulatory**	45572	cAMP	IPI00169788	1900	108	31	422
B3	Bead05	cGMP-dependent protein kinase type Iα (PKG Iα)	76336	cGMP	IPI00458024	2236	76	42	1004
B4	Bead15	Alpha crystallin B-chain	20051	Actin/Cytoskel.	IPI00138274	482	9	9	2228
B5	Bead11	Glyceraldehyde-3-phosphate dehydrogenase (GAPDH)	35661	NAD/NADH	IPI00462301	567	16	9	2229
B6	Bead08	**cAMP-dependent protein kinase type IIß Regulatory**	46019	cAMP	IPI00224570	578	17	10	2707
B7	Bead19	Nucleoside diphosphate kinase A (NDPK A)	17190	AMP/ADP/ATP	IPI00131459	379	6	6	2865
B8	Bead19	Nucleoside diphosphate kinase B (NDPK B)	17466	AMP/ADP/ATP	IPI00127417	498	6	6	2911
B9	Bead07	ATP synthase α-chain	59736	AMP/ADP/ATP	IPI00130280	972	19	17	3144
B10	Bead19	Nucleoside diphosphate kinase 3 (NDPK 3)	19081	AMP/ADP/ATP	IPI00125450	323	6	6	3180
B11	Bead11	L-lactate dehydrogenase A-chain	36350	FAD	IPI00319994	462	11	9	3305
B12	Bead07	Tubulin ß-5 chain	49653	GMP/GDP/GTP	IPI00117352	534	15	9	3310
B13	Bead02	**AKAP2 (AKAP-KL) (Isoform PALM2-AKAP2)**	126072	PKA	IPI00649060	1612	37	33	3407
B14	Bead11	**AKAP7 (AKAP18, AKAP15) isoform γ or δ**	35426	PKA	IPI00380299	319	10	10	3543
B15	Bead05	Heat shock cognate 71 kDa protein	70855	AMP/ADP/ATP	IPI00323357 IPI00480560	961	19	16	3729
B16	Bead06	**Microtubule-associated protein 2 (MAP2) Isoform c or d**	52658	PKA	IPI00653404	571	14	12	3761
B17	Bead09	Actin, alpha skeletal/cardiac/smooth muscle	42034	AMP/ADP/ATP	IPI00114593	483	11	9	3821

Table 1 (Continued)

B18	Bead09	3-ketoacyl-CoA thiolase, mitochondrial	41840	CoA	IPI00117043 IPI00110827 IPI00480406 IPI00226430 IPI00653158	547	10	9	4184
B19	Bead08	Elongation factor 1-alpha 1	50295	GMP/GDP/GTP	IPI00307837	531	11	11	4572
B20	Bead09	Phosphoglycerate kinase 1	44519	GAPDH	IPI00230002	312	9	6	4947
B21	Bead08	Trifunctional enzyme ß-subunit	51370	CoA	IPI00626102 IPI00115607	389	10	8	5137
B22	Bead14	Myosin light polypeptide 3	22273	Myosin	IPI00133392	246	4	4	5568
B23	Bead17	Heat shock protein, alpha-crystallin-related, B6	17503	Actin/Cytoskel.	IPI00652860	156	3	3	5834
B24	Bead06	Acyl-CoA dehydrogenase, very-long-chain specific	71096	CoA	IPI00119203	650	12	12	5925
B25	Bead09	Isocitrate dehydrogenase 2	50889	FAD	IPI00318614	349	8	6	6361
B26	Bead06	Pyruvate kinase, muscle	57986	AMP/ADP/ATP	IPI00407130	373	9	6	6443
B27	Bead02	Myosin heavy chain, cardiac muscle α-isoform	223553	AMP/ADP/ATP	IPI00122737 IPI00129404 IPI00468630	1878	34	33	6575
B28	Bead14	Triosephosphate isomerase	26563	GAPDH	IPI00467833	252	4	4	6641
B29	Bead12	Prohibitin-2	33280	Other/Unknown	IPI00321718	243	5	5	6656
B30	Bead02	**AKAP11 (AKAP220)**	208441	PKA	IPI00125322	1338	31	26	6724
B31	Bead05	Trifunctional protein, α-subunit	82627	CoA	IPI00223092	702	12	11	6886
B32	Bead04	Heat shock protein 1ß	83208	AMP/ADP/ATP	IPI00229080	601	12	10	6934
B33	Bead07	Tubulin α	50118	GMP/GDP/GTP	IPI00604879 IPI00652705 IPI00652850 IPI00403810	383	7	7	7160
B34	Bead12	Heterogeneous nuclear ribonucleoprotein A1	34260	RNA/DNA	IPI00224251 IPI00480230 IPI00553777 IPI00555007	318	4	4	8565
B35	Bead06	60 kDa heat shock protein	60939	AMP/ADP/ATP	IPI00461249 IPI00308885	294	7	5	8706
B36	Bead11	Malate dehydrogenase, mitochondrial precursor	35579	NAD/NADH	IPI00323592 IPI00331590	158	4	3	8895
B37	Bead09	Acyl-CoA dehydrogenase, medium-chain specific	46464	CoA	IPI00134961	165	5	4	9293
B38	Bead10	Aspartate aminotransferase	47394	Other/Unknown	IPI00117312	331	5	5	9479
B39	Bead10	Isocitrate dehydrogenase [NAD] subunit α	39621	NAD/NADH	IPI00459725	189	4	4	9905
B40	Bead06	T-complex protein 1, α-subunit B	60432	Actin/Cytoskel.	IPI00459493	290	6	6	10072
B41	Bead03	**AKAP1 (D-AKAP1) isoform c or d**	92147	PKA	IPI00115506 IPI00230591	462	9	8	10239
B42	Bead05	**AKAP10 (D-AKAP2)**	73615	PKA	IPI00135233	380	7	6	10516
B43	Bead07	**cAMP-dependent protein kinase type Iß Regulatory**	43075	cAMP	IPI00310841	418	4	3	10769
B44	Bead04	Endoplasmin precursor (HSP90-like)	92461	Other/Unknown	IPI00129526	418	8	7	11558
B45	Bead11	Fructosamine-3-kinase	35015	AMP/ADP/ATP	IPI00111519	132	3	2	11672
B46	Bead09	Creatine kinase, sarcomeric	47457	AMP/ADP/ATP	IPI00120076	128	4	3	11864
B47	Bead09	Elongation factor Tu	49491	GMP/GDP/GTP	IPI00625588 IPI00274407	188	4	4	12373
B48	Bead10	Fructose-bisphosphate aldolase A	39207	GAPDH	IPI00221402	148	3	3	13069
B49	Bead05	Heat shock protein 1A or 1B	70077	AMP/ADP/ATP	IPI00123794 IPI00346073	486	5	5	14015
B50	Bead06	T-complex protein 1, delta subunit	57919	Actin/Cytoskel.	IPI00116277	221	4	4	14480
B51	Bead04	Similar to Plakophilin 2	88030	Other/Unknown	IPI00132134	326	6	6	14672
B52	Bead05	Stress-70 protein	73511	AMP/ADP/ATP	IPI00133903	284	5	5	14702
B53	Bead06	T-complex protein 1, theta subunit	59407	Actin/Cytoskel.	IPI00469268	193	4	4	14852
B54	Bead06	T-complex protein 1, eta subunit	59635	Actin/Cytoskel.	IPI00331174	168	4	4	14909
B55	Bead04	Elongation factor 2	95167	GMP/GDP/GTP	IPI00466069	294	6	6	15861
B56	Bead02	**AKAP5 (AKAP79/AKAP150)**	76852	PKA	IPI00339766	290	4	4	19213
B57	Bead06	T-complex protein 1, zeta subunit	57856	Actin/Cytoskel.	IPI00116281	170	3	3	19285
B58	Bead02	Myosin binding protein C, cardiac	141377	AMP/ADP/ATP	IPI00118316	420	7	7	20197
B59	Bead06	Serine/threonine protein phosphatase 2A, 65 kDa regulatory	65175	Other/Unknown	IPI00310091	146	3	3	21725
B60	Bead05	Heterogeneous nuclear ribonucleoprotein M	77633	RNA/DNA	IPI00132443	165	3	3	25878
B61	Bead02	Myomesin 1 protein	175434	AMP/ADP/ATP	IPI00626655 IPI00470145 IPI00281109	284	4	4	43859
B62	Bead02	**AKAP13 (AKAP-Lbc)**	303522	PKA	IPI00126181	398	6	6	50587

[a] (A) Top 20 of proteins identified in the ADP-eluted fraction (sorted by F_{abb}), remainder of ADP eluting proteins are depicted in the Supplemental Table 1. (B) Proteins identified in the cGMP-eluted fraction with >3 unique peptides. (C) Proteins identified in the final enriched fraction (>3 unique peptides/protein). In bold are proteins of particular interest as they directly or indirectly bind to cAMP at physiological conditions. Proteins depicted in gray are found in other lanes with higher abundance. Depicted are MASCOT protein scores based on all peptides with an individual peptide score of 29 or higher ($p < 0.05$) assigned to a protein. Also depicted are number of queries (i.e., number of identified spectra) and amount of unique spectra assigned to a protein with a confidence of 95% or higher, data obtained by Scaffold.

but not to any of the AKAP2 entries in the Swiss-Prot database, reiterating there is an inconsistency between the AKAP2 sequences in the different databases. Nine detected peptides could not be assigned to any of the entries for AKAP2 in both the Swiss-Prot and IPI-mouse databases but did match *Protein*. The peptides originated from the N-terminal domain of *Protein*, between AA 64−244, see Figure 4 and supplemental Figure 1 (Supporting Information). BLAST analysis of AA 1−244 of *Protein* revealed that AA 64−180 had 100% sequence identity with a sequence found in a mouse protein called *Similar to paralemmin 2* (Q8BR92 (TrEMBL), PALM2). The genes of AKAP2 and PALM2 are close together on the same chromosome, and the presence of mRNA coding for an unusual fusion protein that consists of a partial PALM2 sequence and the complete sequence of AKAP2 has been described;[33] however, at the protein level it was never observed. We now ensure the

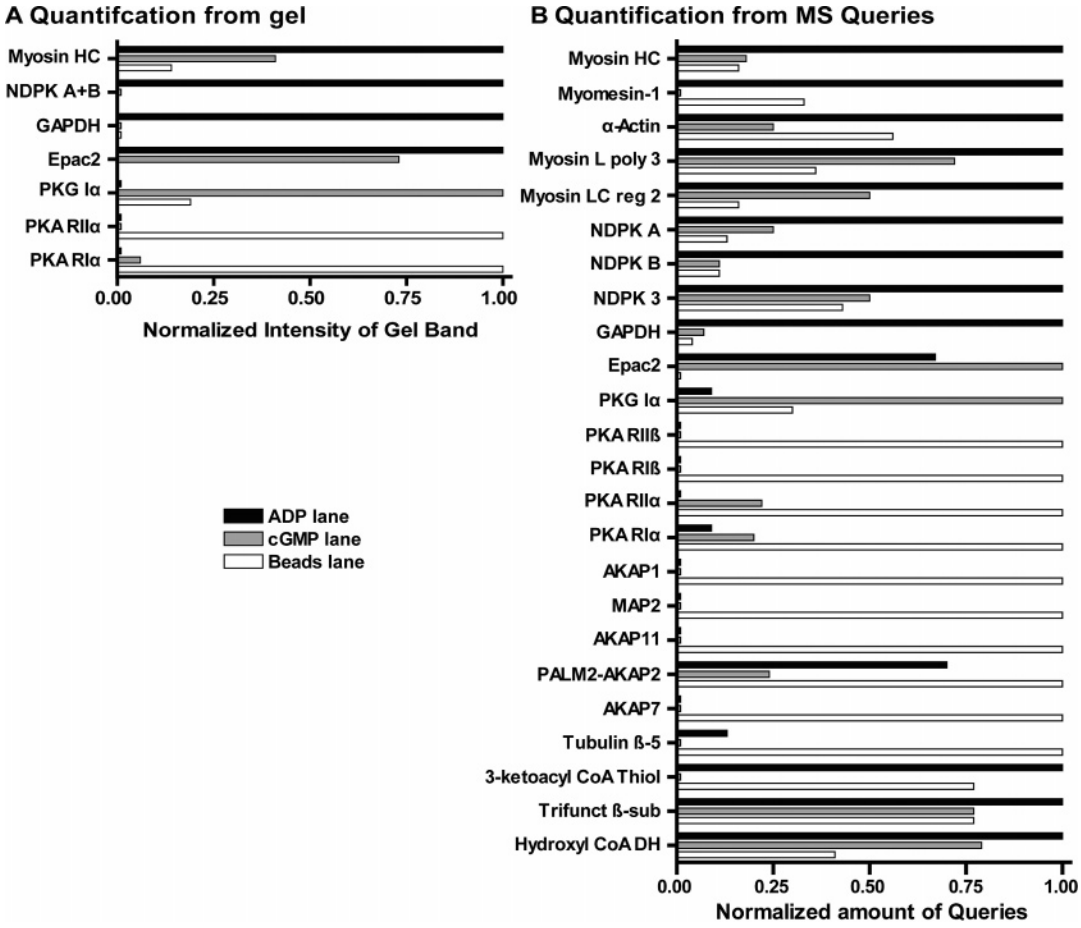

Figure 3. Densiometric quantification *versus* mass spectrometry-based quantification. (A) In gel quantification by densitometry was achieved for several proteins. Intensities are normalized to the highest intensity of a protein in a particular lane. (B) Quantification of proteins in each lane by normalizing the amount of mass queries for a particular protein in each lane to the highest amount.

existence of this fusion protein PALM2-AKAP2. Its presence in our pull down, at an apparent mass between 120 and 160 kDa (band2) in the PKA-R-enriched fraction, strongly suggests this protein retains its AKAP properties and is expressed in heart tissue. The regular PALM2 protein itself is a protein of only 35 kDa. In this molecular weight region of the gel, we did not detect any PALM2 peptides, corroborating the presence of the novel fusion protein PALM2-AKAP2 on the beads.

Of the three so far not discussed unique peptides of *Protein*, one originated from the 124 amino acid stretch that distinguishes the A-isoforms from the B-isoforms of AKAP2 (AA 245−369). Two more peptides were observed at the C-terminus, one in the domain that is present in both KL1 and KL2, but not in KL3 (AA 1039−1092) and another one in a region that is specific for KL1 (AA 1092−1106). Hu et al. suggested that the C-terminal part of PALM2-AKAP2 is possibly similar spliced as the earlier described AKAP2 proteins. From our data we conclude that in mouse ventricular tissue several splice variants of AKAP2 are present, including the fusion protein PALM2-AKAP2. Our analysis does not exclude the possible presence of the "regular" AKAP2 species in our pull down experiment, in fact at least one of the "regular" AKAP2 type A-species is present, as derived from a detected unique N-terminal acetylated peptide.

Interestingly, an interaction between (PALM1) and the dopamine D3 receptor (D3R) has been reported, which induces a reduction of cellular cAMP levels.[34] We speculate that the PALM2-AKAP2 protein might be involved in such pathways, as AKAPs are known to interact often with membrane receptors.[2]

Other Detected AKAPs. AKAP7 (B14) is also abundant in our pull down. Four splice variants of AKAP7 (i.e., AKAP15/AKAP18) have been described; α, β, γ, and δ.[35] The first two are relatively small proteins (15 and 18 kDa, respectively) and contain a membrane targeting domain; the latter two lack this domain but are larger (close to 40 kDa). We detected AKAP7 in a 1D gel band with an apparent mass of 40 kDa (Figure 2, band 11), indicating that we enriched the γ or δ isoforms. Several peptides specific for these two isoforms confirmed this finding. Henn et al. showed a high occurrence of the δ-isoform mRNA in rat heart tissue,[35] but unfortunately our data did not enable us to distinguish between these two larger isoforms.

Also present in our pull-down is MAP2 (B16).[36−38] Four splice variants have been described, MAP2a and MAP2b (270 and 280 kDa, respectively), and two with lower molecular weights: MAP2c (49 kDa) and MAP2d (52 kDa). Most detected peptides originated from a gel band at an apparent mass of 75 kDa, indicating that we are dealing with either MAP2c or MAP2d. We detected 1 peptide uniquely present in MAP2d. By the presence of this peptide, we hypothesize that isoform MAP2d is present in our pull-down. No unique peptides from MAP2c were detected.

We also detected AKAP1 (B41, D-AKAP1) and AKAP10 (B42, D-AKAP2), which are dual specificity AKAPs as they can bind both to PKA RI and RII.[41−43] AKAP1 has at least four

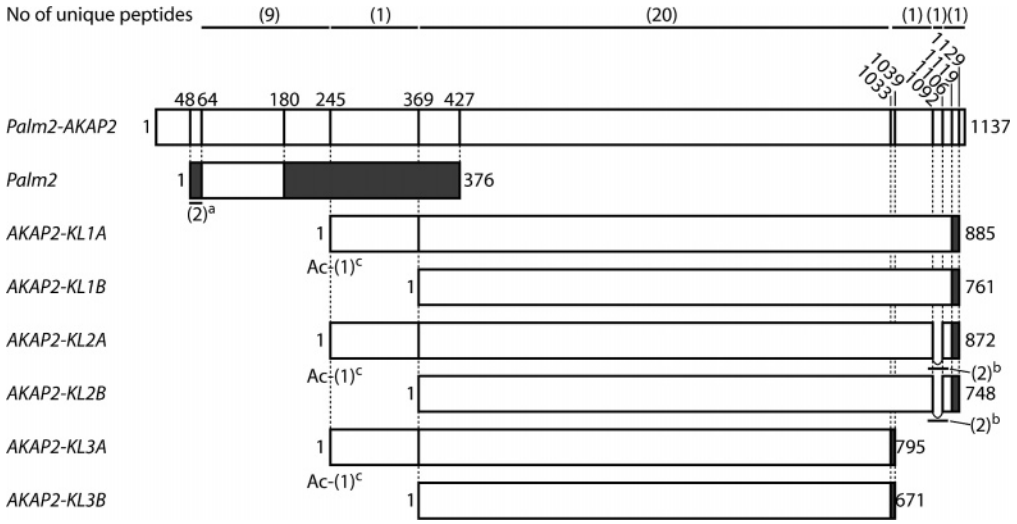

Figure 4. Alignment of PALM2-AKAP2 with PALM2 and AKAP2 isoforms. Sequence alignment of *Protein* (IPI00649060, PALM2-AKAP2) with a mouse protein from the TrEMBL-database called *Similar to PALM2* (Q8BR92) and *AKAP2-KL1A* (O54931), *AKAP2-KL2A* (O54931−2), *AKAP2-KL3A* (O54931−3) from the Swiss-Prot database. Also depicted are the AKAP2-KL B-isoforms, which are formed by an alternate initiation at M125 of their corresponding A-isoforms.[31] All sequences with 100% sequence identity to PALM2-AKAP2 are depicted in white, whereas sequences that are absent in PALM2-AKAP2 are depicted in grey. Also depicted, at the top, are the number of unique peptides identified in the different specific domains of PALM2-AKAP2. In brackets, the number of unique peptides in specific regions of PALM2-AKAP2. [a]Two peptides assigned to PALM2 only. [b]Two peptides observed only in type 2 AKAP2 splice isoforms. [c]Acetylated peptide, representing the earlier described AKAP2-A-isoforms.[31]

Table 2. Site-Specific Detection of Protein Phosphorylation[a]

no.	protein	residues	sequence	$M_{r\,found}$	$M_{r\,expt}$	$M_{r\,calc}$	MASCOT
1	PKA-RIIα	95−115	(R)-RV**p**SVCAETFNPDEEEEDNDPR-(V)	863.346	2587.016	2587.017	50
2	PKA-RIα	71−92	(K)-TGIRTDSREDEI**p**SPPPPNPVVK-(G)	828.748	2483.222	2483.206	54
3	PKA-RIα	71−92	(K)-TGIRTD**p**SREDEIpSPPPPNPVVK-(G)	828.746	2483.215	2483.206	48
4	PKA-RIα	71−92	(K)-TGIRTD**p**SREDEI**p**SPPPPNPVVK-(G)	855.402	2563.184	2563.172	58
5	PKA-RIα	75−92	(R)-TDSREDEI**p**SPPPPNPVVK-(G)	1028.989	2055.964	2055.951	69
6	PKA-RIα	79−92	(R)-EDEI**p**SPPPPNPVVK-(G)	799.383	1596.751	1596.744	97

[a] Some peptides were observed in different charge states, whereby we only considered the one with the highest peptide MASCOT score. Peptide 2 and 3 were observed at the same *m*/*z*, but with different retention times. The MS/MS spectra revealed them to be two distinct peptides, as shown in this table.

splice variants, AKAP1a−d. AKAP1a is the shortest and AKAP1b (S-AKAP84) and 1d (AKAP100) have an additional N-terminal domain, which ensures localization to the endoplasmic reticulum. AKAP1c (AKAP121) and 1d have an extended C-terminal domain.[44,45] From two detected peptides in the C-terminal part of AKAP1 we confirmed the presence of type 1c or 1d. AKAP10 (D-AKAP2) was identified by Wang et al.[46] in heart and many other tissues.

mRNA measurements have indicated that AKAP11 (B30), also named AKAP220, is present in testis,[47] but also in heart.[48] AKAP5, called AKAP150[49] in mice, AKAP75[50] in bovine, and AKAP79[51] in human is mainly found in brain extracts, where it is part of a multi-protein complex around the AMPA[52] and NMDA receptors,[53] as well as at the KCNQ2 potassium channel.[54] Recently, its function in the regulation of cardiac L-Type Ca^{2+}-channels by PKA phosphorylation has been established.[55] AKAP13, also named Ht31, was first described by Carr et al. as a protein originating from a human heart cDNA library.[50,56,57] Later, a much larger protein was cloned, containing the Ht31 sequence, AKAP-Lbc. AKAP-Lbc was shown to be a functional GEF of the GTPase Rac in the formation of stress fibers.[58] AKAP-Lbc has been reported to be expressed in human heart and, to a lower extent, in lung and placenta.[58] Due to our high stringency for protein identification confidence, two detected AKAPs were filtered out. Nonetheless, we mention them here. Both AKAP9 and SKIP (Sphingosine kinase type 1 interacting protein) were detected, albeit with only two unique peptides. These two AKAPs have been described previously to be present in heart tissue. AKAP9 or Yotiao[59] has a specific function in cardiomyocytes and targets PKA, and other signaling molecules to potassium channels to regulate the intracellular potassium concentration.[8] The latter has only recently been acknowledged as an AKAP and was found in heart, but its function, besides anchoring PKA and sphingosine kinase type 1, is largely unknown.[20,60]

***In vivo* Phosphorylation of PKA-R.** Our method provides a sensitive, fast, and robust enrichment for all isoforms of the regulatory subunits of PKA and may be applied directly to any tissue sample, enabling the investigation of *in vivo* phosphorylation. It has been described that PKA-R can be phosphorylated at several positions, also through autophosphorylation.[61,62] Although we did not specifically enrich for phosphopeptides,[23,63] we observed the presence of several interesting phosphopeptides of PKA-RIα and RIIα. The tandem-MS spectra of these phosphopeptides were scrutinized and compared one-to-one with their nonphosphorylated counterparts. Manually approved PKA-R phosphopeptides from our data set are listed in Table 2. For PKA RIα, five phosphopeptides were detected, and for PKA RIIα, one was detected. By creating selected ion chromatograms (SIC) of specific peptides of interest at their observed precursor masses (see Methods), we were able to estimate the relative stoichiometries of phosphorylation.

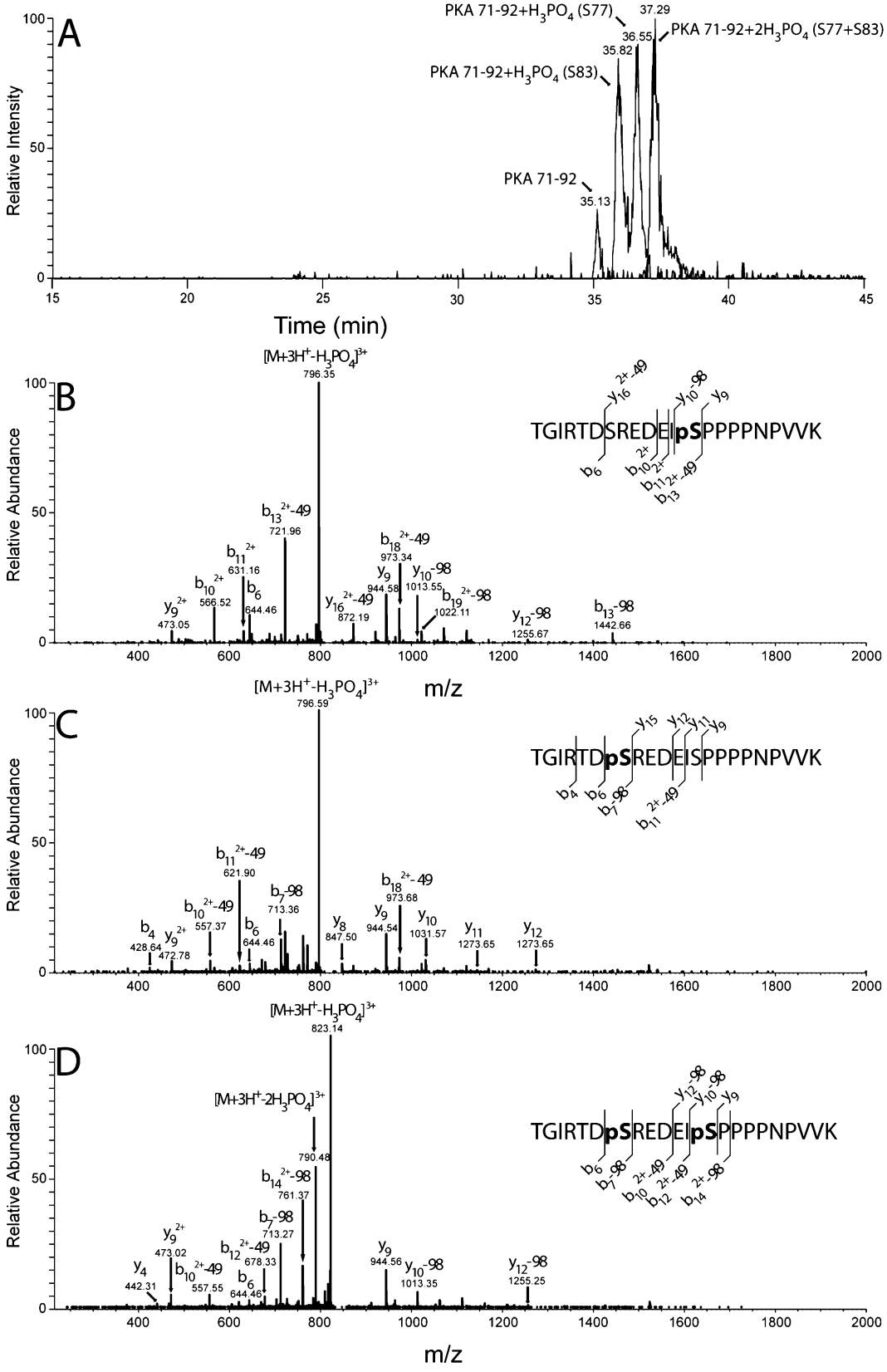

Figure 5. Tandem MS spectra of a differentially phosphorylated peptide of PKA. (A) Overlaid single ion chromatograms (SICs) of PKA RIα-peptide 71−92 in the non-, singly, and doubly phosphorylated form. SICs were generated with precursor masses of the 3^+ ions at *m*/*z* 802.09, 828.74, and 855.40 ± 0.02 Da, respectively. (B) MS/MS spectrum corresponding to peak at 35.82 min. (C) Tandem MS spectrum of peak at 36.55. (D) MS/MS spectrum of doubly phosphorylated peptide with a retention time of 37.29 min. Also depicted are observed *b*- and *y*-ions that were crucial for the annotation of the phosphate group at the specified position(s) in the differentially modified peptide 71−92.

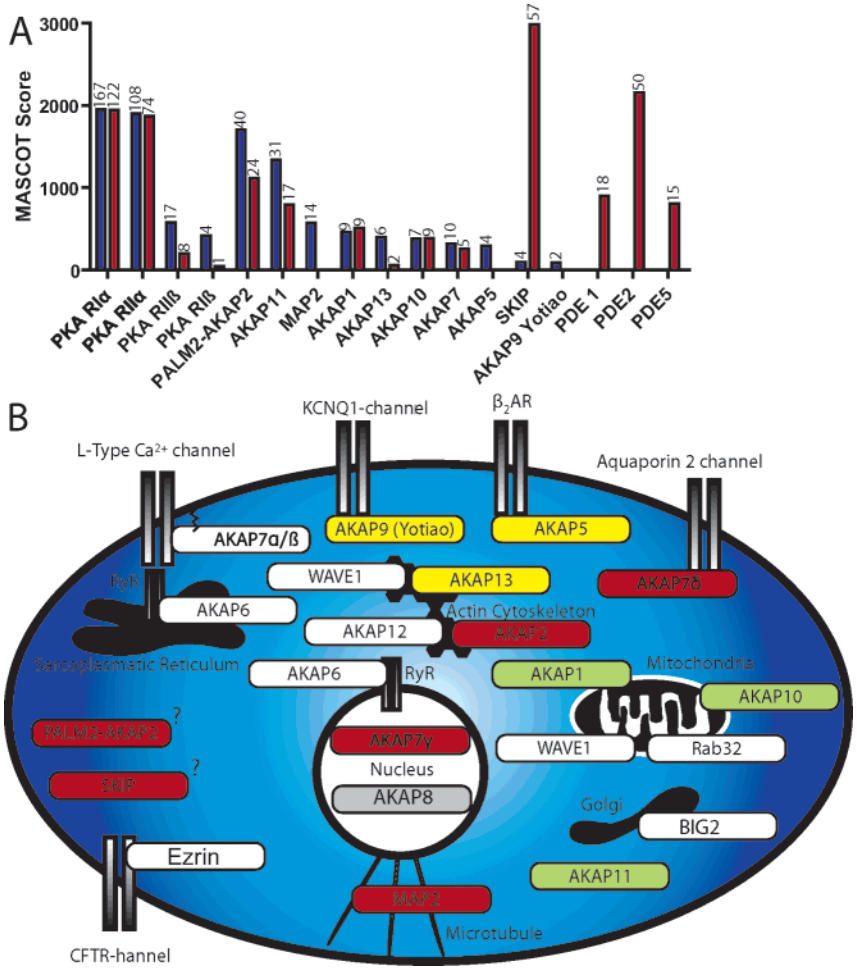

Figure 6. AKAPs identified in heart. (A) Comparing sequence coverage of several proteins pulled down with 8-AEA-cAMP and 2-AH-cGMP in mouse (blue) and rat (red) ventricular tissue, respectively. Sequence coverage measured by MASCOT protein scores (bars) and amount of queries (numbers on top). (B) Heart AKAPs and their subcellular localization. Adapted from Kapiloff et al., Ruehr et al., and Wong et al.[2,71,72] AKAPs identified in this experiment are depicted in red when abundantly present in our PKA-enriched fraction (among top 25 proteins based on F_{abb}), in green proteins in the top 50, but not top 25, and in yellow the lower abundant AKAPs of our pull down. AKAPs in white were not detected in this experiment but were previously reported to be present in heart. A question mark is depicted when the intracellular localization is currently unknown. (KCNQ1, delayed rectifier potassium channel; RyR, ryanodine receptor; β2AR, type 2 β-adrenergic receptor; BIG2, brefeldin A inhibited GEP2.)

Most interesting are the observed peptides originating from amino acids 71−92 of PKA RIα in the non-, singly, and doubly phosphorylated form, as shown in Figure 5. In Figure 5A, the selected ion chromatograms (SIC) of different peptides are overlaid. As shown in this figure, the nonphosphorylated peptide eluded before the singly phosphorylated peptide that eluted with two different retention times. Finally, the doubly phosphorylated peptide eluted. Corresponding tandem-MS spectra of each of these phosphopeptides are shown in Figure 5B−D. These spectra reveal that peptide 71−92, which, in theory, can be phosphorylated at four positions (Thr71, Thr75, Ser77 and Ser83), is actually phosphorylated at either Ser83 (Figure 5B) or Ser77 (Figure 5C) or at both (Figure 5D). This indicates that at least four differently phosphorylated PKA RIα species are present *in vivo* in mouse heart tissue. Based on SIC-quantitation, these occur at roughly the same concentration (Figure 5A).

For PKA RIα, as far as we know, no autophosphorylation sites have been described. Therefore, the phosphorylation sites identified in this experiment are most likely generated by other kinases *in vivo*. Recently, both these phosphorylation sites were identified in a large phosphoproteomics screen for synaptic proteins by Collins et al.,[64] who identified the exact same peptide as we observed (peptide 4, Table 2). Our experiment, however, also reveals that the phosphorylation at these sites is quite dynamic as we also found the nonphophorylated peptide, as well as peptides with individual phosphorylations on Ser77 and Ser83. Ser83 phosphorylation was earlier identified in bovine heart.[65]

The bioinformatics tool NetPhosK (www.cbs.dtu.dk/services/NetPhosK[66]) can predict a match between an observed phosphorylation site and the potential kinase responsible for it. It does this by comparing the sequence around the phosphorylation site to a database of known kinase consensus motifs. NetPhosK analysis of our data revealed a possible involvement of glycogen synthase kinase 3 for Ser83. The other site could not be assigned by NetPhosK. Interestingly, phosphorylation of PKA RII by glycogen synthase kinase has been described earlier.[67]

On PKA RIIα we observed one specific phosphorylation site at Ser97. This site was earlier identified as an autophosphorylation site that reduces the affinity of the regulatory subunit

for the catalytic subunit, thereby prolonging the cAMP signal when intracellular concentrations start to drop.[62,68] Apparently, this autophosphorylation is quite common *in vivo*, as roughly 50% of PKA-RIIα was found phosphorylated at this site, as determined by SIC-based quantitation (data not shown).

Comparing Mouse and Rat Ventricular Tissue with Cyclic Nucleotide Affinity-Based Chemical Proteomics. In a previous chemical proteomics study using immobilized cGMP rather than cAMP as bait and rat ventricular tissue instead of mouse, we also identified all 4 isoforms of PKA-R. Based on the sequence coverage, the enrichment of PKA-R was slightly better in the cAMP-pull down, as expected. The same pattern is observed for the AKAPs in both ventricular tissues.[20] In our current approach with cAMP, we identify the same 7 AKAPs (AKAP1, AKAP2, AKAP7, AKAP10, AKAP11, AKAP13, and SKIP). All but one (SKIP) had slightly more sequence coverage in mouse, as judged by their amount of queries and MASCOT scores (Figure 6).[69] Three AKAPs were only observed in mouse, MAP2, AKAP5, and Yotaio.

One of the most striking differences was the retention of SKIP, which was much less efficient in mouse than in rat. Perhaps the SKIP concentration in rat heart is higher than in mouse, but it is also likely that the retention of SKIP through PKA-R is sterically less favorable when it interacts with a cyclic nucleotide anchored in the 8-position. (In the rat study, 2-AH anchored cGMP was used.) Phosphodiesterase 5 (PDE5) was not pulled down in the mouse experiment, which can be explained by the fact that PDE5 is a cGMP-specific PDE. In addition, PDE1 and PDE2, which are both dual specific PDE's, are likely not present in the mouse pull down with cAMP due to the position of the spacer. PDE's are known to have a crucial interaction with cyclic nucleotides (cGMP or cAMP) around the 8-position; hence, a substituent at that position will hamper PDE interaction with the beads all together.[70]

Then there is the earlier observed presence of PALM2-AKAP2 in this mouse sample. Closer investigation of our earlier rat data[20] revealed the presence of 4 unique PALM2 peptides in the gel band that also contained AKAP2. As in this mouse experiment, no PALM2 peptides were observed around 40 kDa, indicating that the fusion protein PALM2-AKAP2 is also present in rat ventricular tissue.

The phosphorylation states of PKA-RIα and RIIα between mouse and rat heart were also compared. We observed the same peptides, with equal phosphorylation patterns on PKA-RIα, reiterating the further complexity introduced by phosphorylation on the different PKA-RIα isoform assemblies in the ventricular tissue (data not shown). The conservation of these phosphorylation events through multiple species hints toward their importance in the functioning of PKA in ventricular tissue.

Acknowledgment. Support by The Netherlands Proteomics Centre (www.netherlandsproteomicscentre.nl) is gratefully acknowledged. This study was financially supported by The Netherlands Organization for Scientific Research (NWO, Grant No. 916.36.012, TvV). M. Pinkse is kindly acknowledged for technical support.

Supporting Information Available: Additional proteins identified in the ADP eluted fraction (Supplemental Table 1) and sequence alignments (Supplemental Figure 1). This material is available free of charge via the Internet at http://pubs.acs.org.

References

(1) Taylor, S. S.; Kim, C.; Vigil, D.; Haste, N. M.; Yang, J.; Wu, J.; Anand, G. S. Dynamics of signaling by PKA. *Biochim. Biophys. Acta* **2005**, *1754*(1−2), 25−37.
(2) Wong, W.; Scott, J. D. AKAP signalling complexes: focal points in space and time. *Nat. Rev. Mol. Cell Biol.* **2004**, *5*(12), 959−970.
(3) Ray, K. P.; England, P. J. Phosphorylation of the inhibitory subunit of troponin and its effect on the calcium dependence of cardiac myofibril adenosine triphosphatase. *FEBS Lett.* **1976**, *70*(1), 11−16.
(4) Solaro, R. J.; Moir, A. J.; Perry, S. V. Phosphorylation of troponin I and the inotropic effect of adrenaline in the perfused rabbit heart. *Nature* **1976**, *262*(5569), 615−617.
(5) Sculptoreanu, A.; Scheuer, T.; Catterall, W. A. Voltage-dependent potentiation of L-type Ca^{2+} channels due to phosphorylation by cAMP-dependent protein kinase. *Nature* **1993**, *364*(6434), 240−243.
(6) Yoshida, A.; Ogura, A.; Imagawa, T.; Shigekawa, M.; Takahashi, M. Cyclic AMP-dependent phosphorylation of the rat brain ryanodine receptor. *J. Neurosci.* **1992**, *12*(3), 1094−1100.
(7) Fink, M. A.; Zakhary, D. R.; Mackey, J. A.; Desnoyer, R. W.; Apperson-Hansen, C.; Damron, D. S.; Bond, M. AKAP-mediated targeting of protein kinase a regulates contractility in cardiac myocytes. *Circ. Res.* **2001**, *88*(3), 291−297.
(8) Marx, S. O.; Kurokawa, J.; Reiken, S.; Motoike, H.; D'Armiento, J.; Marks, A. R.; Kass, R. S. Requirement of a macromolecular signaling complex for beta adrenergic receptor modulation of the KCNQ1-KCNE1 potassium channel. *Science* **2002**, *295*(5554), 496−499.
(9) Fraser, I. D.; Tavalin, S. J.; Lester, L. B.; Langeberg, L. K.; Westphal, A. M.; Dean, R. A.; Marrion, N. V.; Scott, J. D. A novel lipid-anchored A-kinase Anchoring Protein facilitates cAMP-responsive membrane events. *EMBO J.* **1998**, *17*(8), 2261−2272.
(10) Gray, P. C.; Johnson, B. D.; Westenbroek, R. E.; Hays, L. G.; Yates, J. R. 3rd; Scheuer, T.; Catterall, W. A.; Murphy, B. J. Primary structure and function of an A kinase anchoring protein associated with calcium channels. *Neuron* **1998**, *20*(5), 1017−1026.
(11) Kapiloff, M. S.; Schillace, R. V.; Westphal, A. M.; Scott, J. D. mAKAP: an A-kinase anchoring protein targeted to the nuclear membrane of differentiated myocytes. *J. Cell Sci.* **1999**, *112*(Pt 16), 2725−2736.
(12) Ruehr, M. L.; Russell, M. A.; Bond, M. A-kinase anchoring protein targeting of protein kinase A in the heart. *J. Mol. Cell. Cardiol.* **2004**, *37*(3), 653−665.
(13) Landgraf, W.; Hullin, R.; Gobel, C.; Hofmann, F. Phosphorylation of cGMP-dependent protein kinase increases the affinity for cyclic AMP. *Eur. J. Biochem.* **1986**, *154*(1), 113−117.
(14) Pohler, D.; Butt, E.; Meissner, J.; Muller, S.; Lohse, M.; Walter, U.; Lohmann, S. M.; Jarchau, T. Expression, purification, and characterization of the cGMP-dependent protein kinases I beta and II using the baculovirus system. *FEBS Lett.* **1995**, *374*(3), 419−425.
(15) Pelligrino, D. A.; Wang, Q. Cyclic nucleotide crosstalk and the regulation of cerebral vasodilation. *Prog. Neurobiol.* **1998**, *56*(1), 1−18.
(16) Dostmann, W. R. Inhibitors of cyclic nucleotide-dependent protein kinases. In *Handbook of Cellular Signaling*; Bradshaw, D., Ed.; Academic Press: New York, 2003; Vol. 2, Chapter 201, pp 487−493.
(17) Oda, Y.; Owa, T.; Sato, T.; Boucher, B.; Daniels, S.; Yamanaka, H.; Shinohara, Y.; Yokoi, A.; Kuromitsu, J.; Nagasu, T. Quantitative chemical proteomics for identifying candidate drug targets. *Anal. Chem.* **2003**, *75*(9), 2159−2165.
(18) Speers, A. E.; Cravatt, B. F. Chemical strategies for activity-based proteomics. *Chembiochem* **2004**, *5*(1), 41−47.
(19) Daub, H.; Godl, K.; Brehmer, D.; Klebl, B.; Muller, G. Evaluation of kinase inhibitor selectivity by chemical proteomics. *Assay Drug Dev. Technol.* **2004**, *2*(2), 215−224.
(20) Scholten, A.; Veen, T. A. v.; Vos, M. A.; Heck, A. J. Analysis of the cGMP/cAMP interactome using a chemical proteomics approach in mammalian heart tissue validates sphingosine kinase type 1-interacting protein as a genuine and highly abundant AKAP. *J. Proteome Res.* **2006**, *5*(6), 1435−1447.
(21) Wilm, M.; Shevchenko, A.; Houthaeve, T.; Breit, S.; Schweigerer, L.; Fotsis, T.; Mann, M. Femtomole sequencing of proteins from polyacrylamide gels by nano-electrospray mass spectrometry. *Nature* **1996**, *379*(6564), 466−469.

(22) Meiring, H. D.; van der Heeft, E.; ten Hove, G. J.; de Jong, A. P. J. M. Nanoscale LC-MS(n): technical design and applications to peptide and protein analysis. *J. Sep. Sci.* **2002**, *25*(9), 557−568.
(23) Pinkse, M. W.; Uitto, P. M.; Hilhorst, M. J.; Ooms, B.; Heck, A. J. Selective isolation at the femtomole level of phosphopeptides from proteolytic digests using 2D-NanoLC-ESI-MS/MS and titanium oxide precolumns. *Anal. Chem.* **2004**, *76*(14), 3935−3943.
(24) Sanders, S. L.; Jennings, J.; Canutescu, A.; Link, A. J.; Weil, P. A. Proteomics of the eukaryotic transcription machinery: identification of proteins associated with components of yeast TFIID by multidimensional mass spectrometry. *Mol. Cell. Biol.* **2002**, *22*(13), 4723−4738.
(25) Ishihama, Y.; Oda, Y.; Tabata, T.; Sato, T.; Nagasu, T.; Rappsilber, J.; Mann, M. Exponentially modified protein abundance index (emPAI) for estimation of absolute protein amount in proteomics by the number of sequenced peptides per protein. *Mol. Cell. Proteomics* **2005**, *4*(9), 1265−1272.
(26) Kim, E.; Park, J. M. Identification of novel target proteins of cyclic GMP signaling pathways using chemical proteomics. *J. Biochem. Mol. Biol.* **2003**, *36*(3), 299−304.
(27) Van Hoof, D.; Passier, R.; Ward-Van Oostwaard, D.; Pinkse, M. W.; Heck, A. J.; Mummery, C. L.; Krijgsveld, J. A quest for human and mouse embryonic stem cell-specific proteins. *Mol. Cell. Proteomics* **2006**.
(28) www.matrixscience.com.
(29) www.proteomesoftware.com.
(30) Krall, J.; Tasken, K.; Staheli, J.; Jahnsen, T.; Movsesian, M. A. Identification and quantitation of cAMP-dependent protein kinase R subunit isoforms in subcellular fractions of failing human myocardium. *J. Mol. Cell. Cardiol.* **1999**, *31*(5), 971−980.
(31) Dong, F.; Feldmesser, M.; Casadevall, A.; Rubin, C. S. Molecular characterization of a cDNA that encodes six isoforms of a novel murine A kinase anchor protein. *J. Biol. Chem.* **1998**, *273*(11), 6533−6541.
(32) Altschul, S. F.; Madden, T. L.; Schaffer, A. A.; Zhang, J.; Zhang, Z.; Miller, W.; Lipman, D. J. Gapped BLAST and PSI-BLAST: a new generation of protein database search programs. *Nucleic Acids Res.* **1997**, *25*(17), 3389−3402.
(33) Hu, B.; Copeland, N. G.; Gilbert, D. J.; Jenkins, N. A.; Kilimann, M. W. The paralemmin protein family: identification of paralemmin-2, an isoform differentially spliced to AKAP2/AKAP-KL, and of palmdelphin, a more distant cytosolic relative. *Biochem. Biophys. Res. Commun.* **2001**, *285*(5), 1369−1376.
(34) Basile, M.; Lin, R.; Kabbani, N.; Karpa, K.; Kilimann, M.; Simpson, I.; Kester, M. Paralemmin interacts with D3 dopamine receptors: implications for membrane localization and cAMP signaling. *Arch. Biochem. Biophys.* **2006**, *446*(1), 60−68.
(35) Henn, V.; Edemir, B.; Stefan, E.; Wiesner, B.; Lorenz, D.; Theilig, F.; Schmitt, R.; Vossebein, L.; Tamma, G.; Beyermann, M.; Krause, E.; Herberg, F. W.; Valenti, G.; Bachmann, S.; Rosenthal, W.; Klussmann, E. Identification of a novel A-kinase anchoring protein 18 isoform and evidence for its role in the vasopressin-induced aquaporin-2 shuttle in renal principal cells. *J. Biol. Chem.* **2004**, *279*(25), 26654−26665.
(36) Theurkauf, W. E.; Vallee, R. B. Molecular characterization of the cAMP-dependent protein kinase bound to microtubule-associated protein 2. *J. Biol. Chem.* **1982**, *257*(6), 3284−3290.
(37) Vallee, R. B.; DiBartolomeis, M. J.; Theurkauf, W. E. A protein kinase bound to the projection portion of MAP 2 (microtubule-associated protein 2). *J. Cell Biol.* **1981**, *90*(3), 568−576.
(38) Loveland, K. L.; Hayes, T. M.; Meinhardt, A.; Zlatic, K. S.; Parvinen, M.; de Kretser, D. M.; McFarlane, J. R. Microtubule-associated protein-2 in the rat testis: a novel site of expression. *Biol. Reprod.* **1996**, *54*(4), 896−904.
(39) Salvador, L. M.; Flynn, M. P.; Avila, J.; Reierstad, S.; Maizels, E. T.; Alam, H.; Park, Y.; Scott, J. D.; Carr, D. W.; Hunzicker-Dunn, M. Neuronal microtubule-associated protein 2D is a dual a-kinase anchoring protein expressed in rat ovarian granulosa cells. *J. Biol. Chem.* **2004**, *279*(26), 27621−27632.
(40) Sanchez, C.; Diaz-Nido, J.; Avila, J. Phosphorylation of microtubule-associated protein 2 (MAP2) and its relevance for the regulation of the neuronal cytoskeleton function. *Prog. Neurobiol.* **2000**, *61*(2), 133−168.
(41) Haffner, C.; Jarchau, T.; Reinhard, M.; Hoppe, J.; Lohmann, S. M.; Walter, U. Molecular cloning, structural analysis and functional expression of the proline-rich focal adhesion and microfilament-associated protein VASP. *EMBO J.* **1995**, *14*(1), 19−27.
(42) Verde, I.; Vandecasteele, G.; Lezoualc'h, F.; Fischmeister, R. Characterization of the cyclic nucleotide phosphodiesterase subtypes involved in the regulation of the L-type Ca2+ current in rat ventricular myocytes. *Br. J. Pharmacol.* **1999**, *127*(1), 65−74.
(43) Huang, L. J.; Durick, K.; Weiner, J. A.; Chun, J.; Taylor, S. S. Identification of a novel protein kinase A anchoring protein that binds both type I and type II regulatory subunits. *J. Biol. Chem.* **1997**, *272*(12), 8057−8064.
(44) Huang, L. J.; Wang, L.; Ma, Y.; Durick, K.; Perkins, G.; Deerinck, T. J.; Ellisman, M. H.; Taylor, S. S. NH2-Terminal targeting motifs direct dual specificity A-kinase-anchoring protein 1 (D-AKAP1) to either mitochondria or endoplasmic reticulum. *J. Cell Biol.* **1999**, *145*(5), 951−959.
(45) Alto, N.; Carlisle Michel, J. J.; Dodge, K. L.; Langeberg, L. K.; Scott, J. D. Intracellular targeting of protein kinases and phosphatases. *Diabetes* **2002**, *51*(Suppl 3), S385−388.
(46) Wang, L.; Sunahara, R. K.; Krumins, A.; Perkins, G.; Crochiere, M. L.; Mackey, M.; Bell, S.; Ellisman, M. H.; Taylor, S. S. Cloning and mitochondrial localization of full-length D-AKAP2, a protein kinase A anchoring protein. *Proc. Natl. Acad. Sci. U.S.A.* **2001**, *98*(6), 3220−3225.
(47) Lester, L. B.; Coghlan, V. M.; Nauert, B.; Scott, J. D. Cloning and characterization of a novel A-kinase anchoring protein. AKAP 220, association with testicular peroxisomes. *J. Biol. Chem.* **1996**, *271*(16), 9460−9465.
(48) Reinton, N.; Collas, P.; Haugen, T. B.; Skalhegg, B. S.; Hansson, V.; Jahnsen, T.; Tasken, K. Localization of a novel human A-kinase-anchoring protein, hAKAP220, during spermatogenesis. *Dev. Biol.* **2000**, *223*(1), 194−204.
(49) Bregman, D. B.; Bhattacharyya, N.; Rubin, C. S. High affinity binding protein for the regulatory subunit of cAMP-dependent protein kinase II-B. Cloning, characterization, and expression of cDNAs for rat brain P150. *J. Biol. Chem.* **1989**, *264*(8), 4648−4656.
(50) Bregman, D. B.; Hirsch, A. H.; Rubin, C. S. Molecular characterization of bovine brain P75, a high affinity binding protein for the regulatory subunit of cAMP-dependent protein kinase II beta. *J. Biol. Chem.* **1991**, *266*(11), 7207−7213.
(51) Carr, D. W.; Stofko-Hahn, R. E.; Fraser, I. D.; Cone, R. D.; Scott, J. D. Localization of the cAMP-dependent protein kinase to the postsynaptic densities by A-kinase anchoring proteins. Characterization of AKAP 79. *J. Biol. Chem.* **1992**, *267*(24), 16816−16823.
(52) Greengard, P.; Jen, J.; Nairn, A. C.; Stevens, C. F. Enhancement of the glutamate response by cAMP-dependent protein kinase in hippocampal neurons. *Science* **1991**, *253*(5024), 1135−1138.
(53) Colledge, M.; Dean, R. A.; Scott, G. K.; Langeberg, L. K.; Huganir, R. L.; Scott, J. D. Targeting of PKA to glutamate receptors through a MAGUK-AKAP complex. *Neuron* **2000**, *27*(1), 107−119.
(54) Alto, N. M.; Soderling, S. H.; Hoshi, N.; Langeberg, L. K.; Fayos, R.; Jennings, P. A.; Scott, J. D. Bioinformatic design of A-kinase anchoring protein-in silico: a potent and selective peptide antagonist of type II protein kinase A anchoring. *Proc. Natl. Acad. Sci. U.S.A.* **2003**, *100*(8), 4445−4450.
(55) Gao, T.; Yatani, A.; Dell'Acqua, M. L.; Sako, H.; Green, S. A.; Dascal, N.; Scott, J. D.; Hosey, M. M. cAMP-dependent regulation of cardiac L-type Ca2+ channels requires membrane targeting of PKA and phosphorylation of channel subunits. *Neuron* **1997**, *19*(1), 185−196.
(56) Carr, D. W.; Hausken, Z. E.; Fraser, I. D.; Stofko-Hahn, R. E.; Scott, J. D. Association of the type II cAMP-dependent protein kinase with a human thyroid RII-anchoring protein. Cloning and characterization of the RII-binding domain. *J. Biol. Chem.* **1992**, *267*(19), 13376−13382.
(57) Newlon, M. G.; Roy, M.; Morikis, D.; Carr, D. W.; Westphal, R.; Scott, J. D.; Jennings, P. A. A novel mechanism of PKA anchoring revealed by solution structures of anchoring complexes. *EMBO J.* **2001**, *20*(7), 1651−1662.
(58) Diviani, D.; Soderling, J.; Scott, J. D. AKAP-Lbc anchors protein kinase A and nucleates Galpha 12-selective Rho-mediated stress fiber formation. *J. Biol. Chem.* **2001**, *276*(47), 44247−44257.
(59) Schmidt, P. H.; Dransfield, D. T.; Claudio, J. O.; Hawley, R. G.; Trotter, K. W.; Milgram, S. L.; Goldenring, J. R. AKAP350, a multiply spliced protein kinase A-anchoring protein associated with centrosomes. *J. Biol. Chem.* **1999**, *274*(5), 3055−3066.
(60) Lacana, E.; Maceyka, M.; Milstien, S.; Spiegel, S. Cloning and characterization of a protein kinase A anchoring protein (AKAP)-related protein that interacts with and regulates sphingosine kinase 1 activity. *J. Biol. Chem.* **2002**, *277*(36), 32947−32953.

(61) Aitken, A.; Hemmings, B. A.; Hofmann, F. Identification of the residues on cyclic GMP-dependent protein kinase that are autophosphorylated in the presence of cyclic AMP and cyclic GMP. *Biochim. Biophys. Acta* **1984**, *790*(3), 219−225.
(62) Rangel-Aldao, R.; Rosen, O. M. Dissociation and reassociation of the phosphorylated and nonphosphorylated forms of adenosine 3′:5′ -monophosphate-dependent protein kinase from bovine cardiac muscle. *J. Biol. Chem.* **1976**, *251*(11), 3375−3380.
(63) Ficarro, S. B.; McCleland, M. L.; Stukenberg, P. T.; Burke, D. J.; Ross, M. M.; Shabanowitz, J.; Hunt, D. F.; White, F. M. Phosphoproteome analysis by mass spectrometry and its application to Saccharomyces cerevisiae. *Nat. Biotechnol.* **2002**, *20*(3), 301−305.
(64) Collins, M. O.; Yu, L.; Coba, M. P.; Husi, H.; Campuzano, I.; Blackstock, W. P.; Choudhary, J. S.; Grant, S. G. Proteomic analysis of in vivo phosphorylated synaptic proteins. *J. Biol. Chem.* **2005**, *280*(7), 5972−5982.
(65) Boeshans, K. M.; Resing, K. A.; Hunt, J. B.; Ahn, N. G.; Shabb, J. B. Structural characterization of the membrane-associated regulatory subunit of type I cAMP-dependent protein kinase by mass spectrometry: identification of Ser81 as the in vivo phosphorylation site of RIalpha. *Protein Sci.* **1999**, *8*(7), 1515−1522.
(66) Blom, N.; Sicheritz-Ponten, T.; Gupta, R.; Gammeltoft, S.; Brunak, S. Prediction of post-translational glycosylation and phosphorylation of proteins from the amino acid sequence. *Proteomics* **2004**, *4*(6), 1633−1649.
(67) Hemmings, B. A.; Aitken, A.; Cohen, P.; Rymond, M.; Hofmann, F. Phosphorylation of the type-II regulatory subunit of cyclic-AMP-dependent protein kinase by glycogen synthase kinase 3 and glycogen synthase kinase 5. *Eur. J. Biochem.* **1982**, *127*(3), 473−481.
(68) Takio, K.; Smith, S. B.; Krebs, E. G.; Walsh, K. A.; Titani, K. Primary structure of the regulatory subunit of type II cAMP-dependent protein kinase from bovine cardiac muscle. *Proc. Natl. Acad. Sci. U.S.A.* **1982**, *79*(8), 2544−2548.
(69) Kolkman, A.; Olsthoorn, M. M.; Heeremans, C. E.; Heck, A. J.; Slijper, M. Comparative proteome analysis of Saccharomyces cerevisiae grown in chemostat cultures limited for glucose or ethanol. *Mol. Cell. Proteomics* **2005**, *4*(1), 1−11.
(70) Sung, B. J.; Hwang, K. Y.; Jeon, Y. H.; Lee, J. I.; Heo, Y. S.; Kim, J. H.; Moon, J.; Yoon, J. M.; Hyun, Y. L.; Kim, E.; Eum, S. J.; Park, S. Y.; Lee, J. O.; Lee, T. G.; Ro, S.; Cho, J. M. Structure of the catalytic domain of human phosphodiesterase 5 with bound drug molecules. *Nature* **2003**, *425*(6953), 98−102.
(71) Kapiloff, M. S. Contributions of protein kinase A anchoring proteins to compartmentation of cAMP signaling in the heart. *Mol. Pharmacol.* **2002**, *62*(2), 193−199.
(72) Ruehr, M. L.; Russell, M. A.; Ferguson, D. G.; Bhat, M.; Ma, J.; Damron, D. S.; Scott, J. D.; Bond, M. Targeting of protein kinase A by muscle A kinase-anchoring protein (mAKAP) regulates phosphorylation and function of the skeletal muscle ryanodine receptor. *J. Biol. Chem.* **2003**, *278*(27), 24831−24836.

PR060601A